A&A manuscript no.
(will be inserted by hand later)

Your thesaurus codes are:
08 (03.20.8; 08.06.3; 08.09.2; 08.12.1; 08.19.2; 10.05.1)

ASTRONOMY
AND
ASTROPHYSICS
10.11.1996

The surface gravities of cool dwarf stars revisited ⋆

K. Fuhrmann, M. Pfeiffer, C. Frank, J. Reetz, and T. Gehren

Institut für Astronomie und Astrophysik der Universität München, Scheinerstraße 1, 81679 München, Germany

Received date; accepted date

Abstract. On the base of high-resolution spectra and standard model atmosphere analyses we propose to employ the pressure-broadened Mg Ib lines to derive the gravity parameter for F and G stars. These lines are advocated to be a much more robust and reliable tracer compared to the ionization equilibrium of, say, Fe I/Fe II, which is susceptible to overionization effects and uncertainties in the temperature structure of the model atmosphere. It is demonstrated that the strong line method circumvents the long-standing discrepancy ($\Delta \log g$ ∼0.5 dex) of the standard F star *Procyon*, the surface gravity of which is precisely known due to its nearness and binary nature. We also discuss similar effects on other, predominantly metal-poor stars. In fact, many of the F and hotter G stars deviate in the LTE metal abundances of neutral and ionized species by up to 0.2 dex. However, once the surface gravity parameter is fixed, very reliable iron abundances from Fe II can be derived as well. As a consequence a number of stars considered to be standards will require revised stellar parameters in future analyses. This will have some impact on stellar distances, ages, and galactic evolution in particular.

Key words: Techniques: spectroscopic – stars: fundamental parameters – stars: individual: Procyon – stars: late-type – stars: subdwarfs – Galaxy: evolution

1. Introduction

The physics of stellar photospheres aims at both, the detailed understanding of all intrinsic processes that generate the observed spectrum, and – even more – at deriving the stellar input parameters for numerous applications in e.g. galactic research. In that respect, the Sun is a unique laboratory and reference source. Albeit we learn from *direct* observations and the extremely resolved spectrum that our means of modeling are not at all sophisticated, one may nevertheless state that we understand at least the basic processes in the solar photosphere. Along with its precisely known effective temperature and surface gravity, standard model atmosphere analyses for instance result in a remarkably good match of the elemental abundance pattern compared to the meteoritic one derived from carbonaceous C1 chondrites in which most of the abundances of the primeval solar nebula are recorded. At this confidence level there is justified hope to a similar understanding of *stellar* photospheres, at least for solar-type stars and as long as we intend to work differentially. It seems reasonable to restrict the sample to spectral types F and G *on* or *close* to the main sequence and ask whether there are other single-lined standards that provide accurate stellar parameters from direct methods. The answer to this question is "yes", but there is currently only *one* – the F5 star Procyon. It is close by and therefore allows the direct measurement of the stellar diameter. Because of its white dwarf companion it is also possible to derive the stellar mass from astrometric methods. Steffen (1985), among others, has analysed this star at length and found discrepant results from the standard model atmosphere approach in that the surface gravity derived from the ionization equilibrium turns out to be $\log g \approx 3.55$, compared to the direct astrometric value $\log g = \log(GM/R^2) = 4.05$.

A discrepancy of this amount is without doubt not acceptable and has led to the notion that the temperature stratification of the standard hydrostatic model atmosphere approach is erroneous, or that the assumption of local thermodynamic equilibrium is not fulfilled, or both.

Irrespective of this major shortcoming, F stars are of course not excluded from stellar analyses. But this seems risky, unless we can solve or circumvent the contradicting problems we have with Procyon. One might conjecture that many spectroscopists (as well as photometrists) are not aware of these fundamental problems and take model atmospheres and results of so-called standard stars for granted. Kurucz (1995a) e.g. is a good reference for a recent discussion of probable errors that can arise following the "black box" approach.

Send offprint requests to: K. Fuhrmann

⋆ Based on observations collected at the German Spanish Astronomical Center, Calar Alto, Spain

On the other hand, we intend to demonstrate in what follows that the spectrum of Procyon nevertheless contains the unequivocal fingerprints of the *correct* surface gravity value in the framework of standard model atmospheres.

It is well-known since long that strong lines with pronounced wings can be good tracers of the gravity parameter, since stars with extended atmospheres provide much less support for collisional broadening (e.g. Gray 1992, and references therein). Cayrel & Cayrel (1963), for instance, employed the pressure-dependent Mg Ib lines λ5172 and λ5183 in ϵ Virginis (G8III) as gravity indicators, and, more specific, Cayrel de Strobel (1969) presented the Mg Ib triplet lines as one of the best gravity criteria for late-type stars. Later, Blackwell & Willis (1977) derived the $\log g$ parameter of Arcturus (K2 III) from the strong Fe I line λ5269. In combination with weak Fe I lines they proved to be fairly independent of the effective temperature with this method. More recently, Smith, Edvardsson & Frisk (1986) determined the surface gravity parameter from the pressure-broadened Ca I line λ6162 in their analysis of α CenA (G2 V) and α CenB (K0 V), followed by τ Ceti (G8 V) and η CasA (G0 V) in Smith & Drake (1987), the K0 giant Pollux (Drake & Smith 1991), the G8 subdwarf Groombridge 1830 (Smith et al. 1992) and the K2 dwarf ϵ Eridani (Drake & Smith 1993).

Most remarkable, however, is the work of Edvardsson (1988a, 1988b, and references therein), who compared the strong line method to the ionization equilibrium method. His elaborate study made use of strong lines from Fe I and Ca I λ6162 applied to a sample of 8 nearby subgiants with α CenA+B and Arcturus included. As a result, the surface gravities derived from the ionization equilibria of iron and silicon are found to be *systematically lower* than the strong line gravities. This, as Edvardsson proposes, may be an effect of errors in the model atmospheres, or departures from LTE in the ionization equilibria. Since then many abundance analyses of late stars have been done. But except for few investigations – such as those mentioned above – most of them do not take advantage of the wealth of information stored in the wings of strong lines.

By means of the strong Mg Ib lines and in conjunction with other, rather weak, Mg I lines we endorse in what follows that the strong line method is able to earmark the surface gravity in a very reliable way in most F and G dwarfs. This especially holds true since we proceed differentially and therefore a precise knowledge of neither the effective temperature nor metal abundance is required. As a consequence it is also possible to derive a very well established iron abundance from Fe II, the dominant stage of ionization in our temperature range.

In Section 2 we give a short description of the observations. Section 3 discusses the model atmospheres and line formation. We then proceed in Sect. 4 to exemplify with respect to Procyon how we intend to derive stellar parameters in future analyses. Section 5 gives some results for other, predominantly metal-poor stars, followed by the conclusions in the final section.

2. Observations

This is the first paper that is based on observations with the fiber optics cassegrain échelle spectrograph FOCES (Pfeiffer et al. 1996) installed recently at the Calar Alto Observatory in Spain. In short, this device provides a spectral coverage of more than 3000Å (≈70 orders) at a resolving power of up to 37000, if equipped with a 1024^2 24μ CCD (∼68mÅ/pixel at 5500Å). It produces almost no stray-light due to its special *white pupil* configuration. In addition the user benefits very much from a well defined blaze function that leaves little room to personal interaction when determining the continuum, as is illustrated in Fig. 1 and 2 for the rectification of the Hα and Hβ region.

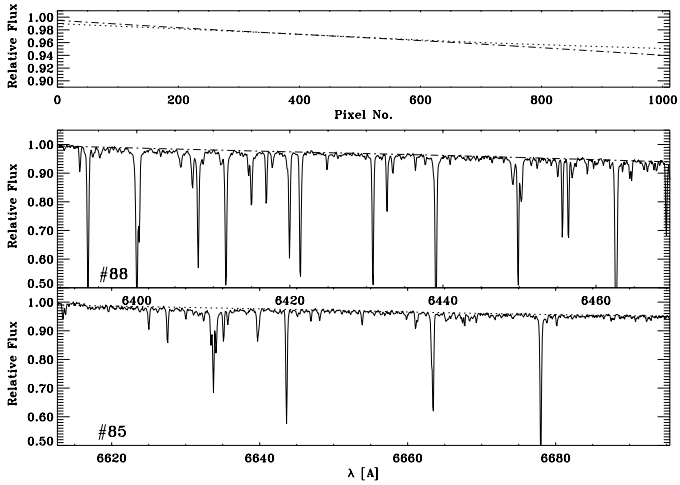

Fig. 1. Rectification of Moon (=reflected sunlight) spectra obtained with the FOCES spectrograph in the region of the Hα line: échelle orders #88 and #85 on the short- and long-wavelength side of the Balmer line show rectification curves that differ by less than 1% (top panel). The continua of the échelle orders 86 and 87 are found by interpolation

The spectra we discuss below have been obtained on the third and last test run in September 1995 at the 2.2m telescope of the Calar Alto Observatory. Although the seeing was not excellent (1.5 to 2.″) and the spectrograph not yet in the final optimized stage, we obtained typical signal-to-noise values of ∼ 100 at 5000Å for a 10th magnitude star within 30 minutes. Table 1 gives a short log of the observations relevant for the next sections. Except for HD 140283, all stars were observed at least twice, with each exposure ranging from 3900 to 6900Å. Signal-to-noise ratios are calculated from Poisson statistics, with a negligible CCD readout contribution. The actual data however show an unexpected residual noise level of 0.5% as a result of moving the fibre position with the telescope. For

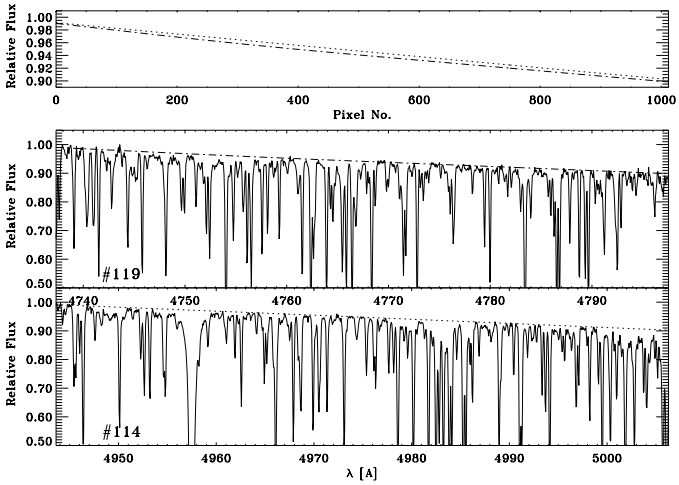

Fig. 2. Same as Fig. 1, but for Hβ: échelle orders #119 on the blue side and #114 on the red side of Hβ are used for interpolation

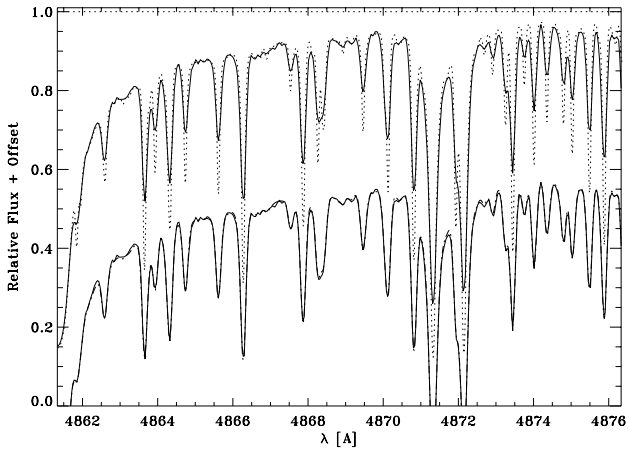

Fig. 3. Comparison of the FOCES Moon spectrum to the Kitt Peak Solar Flux Atlas (dotted curve, renormalized by 0.5% "up"). A Gaussian of 4.6 ± 0.2 km s^{-1} applied to the latter results in the (offset) dot-dashed curve, demonstrating the great similarity of both spectra

Table 1. Log of observations taken with the FOCES échelle spectrograph in September 1995. All spectra cover the range 3900–6900Å. Exposure times are integrated values in seconds. The nominal signal-to-noise ratio is valid around 5500Å

Object	HD	V	Exp. time	S/N (5500Å)
HR 17	HD 400	5.97	720	470
	HD 19445	8.05	3600	300
HR 1545	HD 30743	6.26	1200	550
HR 2943*	HD 61421	0.37	30	550
	HD 140283	7.24	1800	220
HR 7560**	HD 187691	5.11	1200	690
	HD 194598	8.35	2400	350
	HD 201891	7.37	1440	450
Moon			28	720

*Procyon, ** o Aquilae

this reason the *true* S/N values are not better than ∼200. The data reduction follows the common path of e.g. Horne (1986). Details with respect to the FOCES spectrograph and the data reduction will be given in due course (Pfeiffer et al. 1996).

Fig. 3 shows a comparison of the FOCES Moon spectrum at the red wing of Hβ to the Kitt Peak Solar Flux Atlas (Kurucz et al. 1984, dotted curve, here: renormalized by 0.5% "up"), which serves as our primary reference source. Convolution with a Gaussian of 4.6 ± 0.2 km s^{-1} results in the (offset) dot-dashed curve, which clearly reproduces the FOCES data to a high degree.

3. Model atmospheres and line formation

3.1. Model atmospheres

In the context of standard theoretical LTE model atmospheres considerable improvements have been obtained by Kurucz (1995b, and references therein). His new opacity line lists are enormously extended compared to the ones of Kurucz (1979), which have been the standard for more than a decade. Certainly many working groups benefit very much from this work. The model atmosphere program we use (Gehren 1977, Fuhrmann et al. 1993) also rests upon the opacity distribution functions (ODF) issued by Kurucz. In this respect it is interesting to investigate how much the new ODFs influence the temperature structure of the standard solar model.

There is, however, one aspect we have to mention in advance, namely the discussion of the solar iron abundance. Holweger et al. (1990) found log ϵ(Fe)= 7.48, a value considerably lower than log ϵ(Fe)= 7.67, the one proposed by Blackwell et al. (1984) and recommended in Anders & Grevesse (1989). Since then the literature saw a lot of pros and cons (e.g. Holweger et al. 1991, Grevesse 1991, Hannaford et al. 1992, Grevesse & Noels 1993, Milford et al. 1994, Anstee & O'Mara 1995, Blackwell et al. 1995, and references therein), "final" words (Biémont et al. 1991) and arguments against this (Kostik et al. 1996). But in spite of the continued discussion, there is currently a preference to assume the meteoritic value log ϵ(Fe)= 7.51 to be the most probable one and this is also adopted in our analysis. Kurucz (1992b), however, took log ϵ(Fe)= 7.67 for his opacity calculations, because he referred to the compilation of Anders & Grevesse (1989). Thus, compared to the meteoritic value, the iron opacities enter his tab-

ulated ODF files with a systematic offset of +0.16 dex. Were it not this element which is the *dominant* line blanketing contributor to our stellar model atmospheres, this would not cause doubt about the tabulated opacity calculations. Even more, the recent investigation of Bell et al. (1994) has shown that the Kurucz line lists obviously produce *more* absorption lines than are actually observed in the solar spectrum. Of course, those lines which are only *predicted*, can be shifted in wavelength position, but Bell et al. particularly criticize the absence of a *balance* of observed versus predicted lines that is anyhow required.

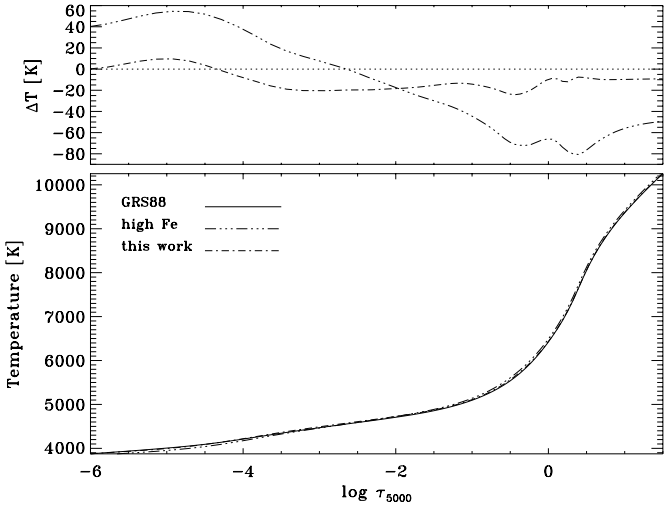

Fig. 4. Atmospheric temperature stratifications vs. optical depth for models with solar parameters T_{eff} = 5780 K and log g = 4.44. Bottom: "GRS88" refers to the old model (cf. Fuhrmann et al. 1993) which employed Kurucz (1979) opacities. The new ODF data result in the model labeled "high Fe". The dot-dashed curve is obtained from ODF-scaling by −0.16 dex (see text). Top: differences in temperature in the sense *GRS88 – high Fe* and *GRS88 – this work* (dot-dashed). All models have been calculated with a mixing-length parameter $\alpha = 0.5$

In this situation we decided not to use the original Kurucz ODFs, but instead to generate *interpolated* ODFs scaled by −0.16 dex, although this scaling inevitably treats *all* elements in the same way. In view of a much faster hardware and with respect to metal-poor stars with their intrinsically non-solar abundance patterns, there can be no doubt that drawbacks of this kind can only be solved by opacity sampling (OS) methods instead of using pretabulated ODFs. Therefore our model atmosphere program is currently revised and tested to allow for this option. For the time being and in what follows we rely however on the ODF approximation and the scaling described above. Note, that this choice does not affect *differential* analyses to first order.

The models recently generated this way either assume relative solar abundances (but scaled by −0.16 dex) or an abundance pattern with α-elements (O, Ne, Mg, Si, S, Ar, Ca and Ti) increased by +0.4 dex. Except for a small grid around Procyon, whose microturbulence parameter is close to 2 km s^{-1}, all calculations were done with ξ_t = 1 km s^{-1} (in the case of Procyon this difference in microturbulence changes the temperature structure by some 30 K).

In Fig. 4 we show the comparison of our old ("GRS88") and new solar model. As is obvious from inspection the model with the new ODFs (labeled "high Fe") results in a slightly steeper temperature gradient, i.e. a model atmosphere that is also somewhat hotter in the deeper layers. Scaling of these opacities by −0.16 dex however reduces the differences to about ∼ 20 K. This is by no means an unexpected result, and since iron produces much of the line blanketing, it addresses the necessity to know its abundance to a very high precision. Although Fig. 4 reveals significant changes as a result of new opacities, a good deal of it is due to the increased solar iron abundance value log ϵ(Fe)= 7.67, compared to log ϵ(Fe)= 7.54 Kurucz used in 1979. Note, however, that this result is claimed only on the grounds of Fig. 4, i.e. for the solar model. A completely different picture can be expected from molecular opacities of cooler stars, where much progress has occurred in recent years.

Very recently Castelli, Gratton & Kurucz (1996) recalculated the solar ATLAS9 model by means of an ODF, where the high iron abundance is replaced by the meteoritic value. There are considerable changes between both models, albeit a second test, in which Castelli et al. scale *all* line opacities by −0.2 dex, also reveals that the integral effect of other elements is obviously more important. The model with the −0.2 dex reduced opacities decreases a gap in the Hβ region of observed and computed fluxes, but conversely introduces discrepancies longward of 5800 Å. These calculations again remind us that line blanketing is a dominant contributor to the atmospheric structure and now as before a source of uncertainties (for recent progress reports in line identifications and calculations see e.g. Nave & Johansson 1993a, 1993b and Kurucz 1995c).

3.2. Line formation

One consequence of the changed structure of the new solar model atmosphere is a slight decrease in the effective temperature value derived from Balmer lines. Whereas our previous models (Fuhrmann et al. 1993) more or less reproduced the observations with 5780 K, the new calculations provide ∼ 5750 K (cf. Fig. 5 and 6). A similar effect is present in the tracings of Procyon as discussed in the next section, but decreases in the models of metal-poor stars.

In view of the fact that the FOCES spectrograph produces spectra that cover a large part of the visual region, and as a result of our new grid of model atmospheres, a completely revised Fe I and Fe II line list of astrophysical oscillator strengths and damping parame-

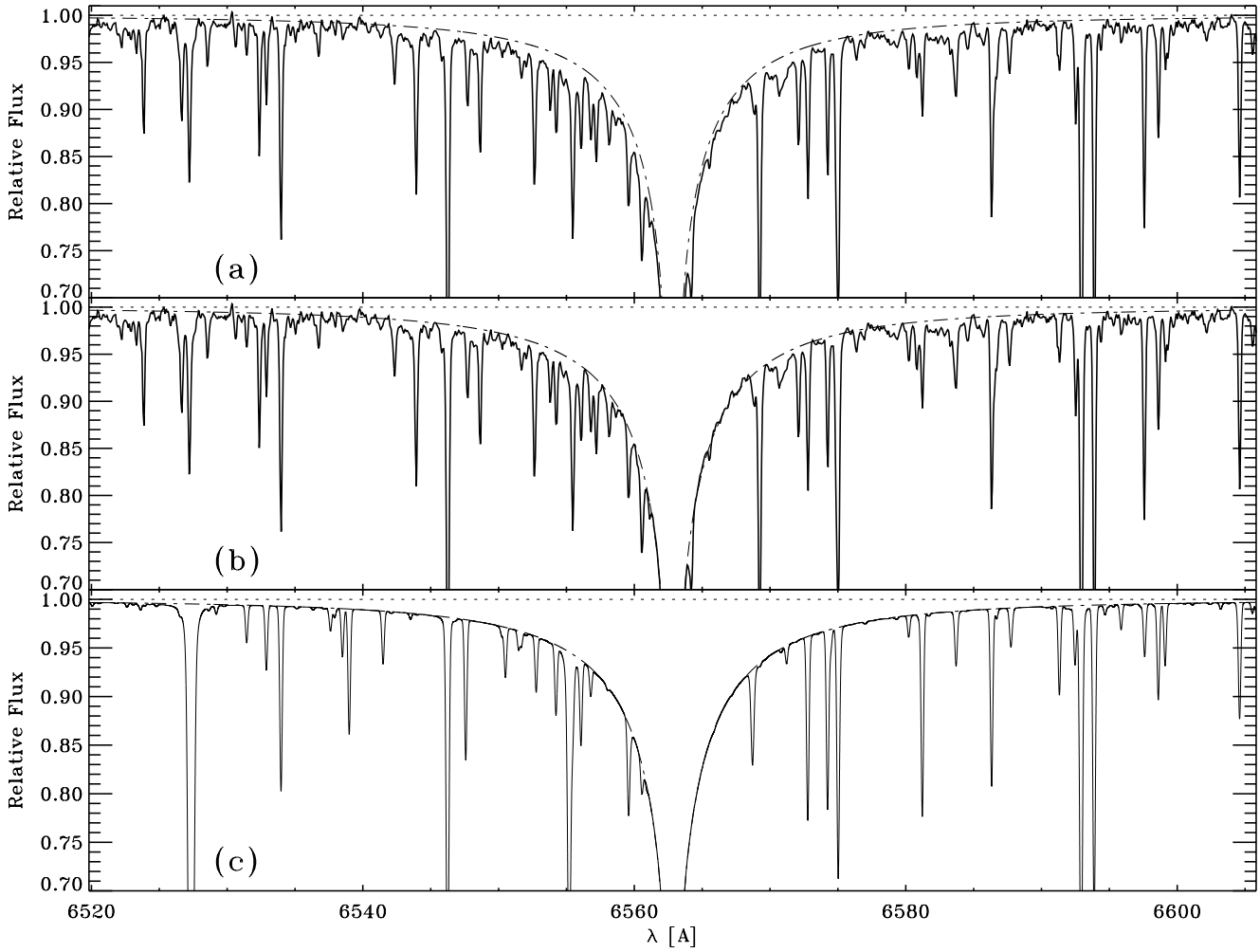

Fig. 5. Balmer line profiles of Hα for two solar models T_{eff} = 5680 K, log g=4.44 (top) and T_{eff} = 5780 K, log g=4.44 (below) compared to the Moon (=reflected sunlight) spectrum. The calculated wings for T_{eff} = 5780 K are slightly too deep, a $\sim$ 30 K lower effective temperature value is indicated. Bottom: spectrum synthesis of $\sim$800 unadjusted, but convolved (rotation, macroturbulence + instrumental profile) metal lines. In spite of existing discrepancies between theory and observation (e.g. Kurucz 1995c for a recent reference) it is most obvious that there is enough information to trace the Balmer line wings of Hα from the "high points" in panel (b)

ters had to be established. All calculations were done in LTE and applied to the Kitt Peak Solar Flux Atlas (Kurucz et al. 1984). For this sample of iron lines (N = 129) we derive a (depth-independent) microturbulence value of $\xi_t = 0.90 \pm 0.15$ km s^{-1}. Rotational broadening is assumed to be 1.7 km s^{-1} and broadening by macroturbulence is taken into account by a radial-tangential profile of ζ_{RT} = 3.3 km s^{-1} for stronger lines, and up to ζ_{RT} = 3.7 km s^{-1} for weak lines (cf. Gray 1977).

Figure 7 compares our astrophysical gf-values to those of Kurucz (1992a). As could have been expected there is considerable scatter in the oscillator strengths, but the *average* scale is practically the same. This is, of course, no striking argument in favour or against a particular value of the solar iron abundance (cf. Sect. 3.1). Our gf-values result from a prespecified temperature structure, turbulence parameters and an adopted solar iron abundance. But, on the other hand, it is interesting to see that our gf-values on average compare to the one of Kurucz *if* we adopt the solar iron abundance to be the meteoritic value.

To apply the method proposed in the next section, we also had to analyse the profiles of the few magnesium lines available in the visible. Most of them possess fairly well-known gf-values, especially the Mg Ib lines, where we directly adopt the absolute oscillator strengths from the literature. Radiation damping constants γ_{rad} are taken from Wiese et al. (1969) and Chang (1990), whereas the damping parameters from van der Waals (C_6) broadening are part of our differential analysis of the Kitt Peak Solar Flux Atlas. Stark effect damping (C_4) has a small influence on the strong lines and is only considered for $\lambda\lambda$5172, 5183 and 5528 (cf. Gray 1992); isotopic wavelength shifts, how-

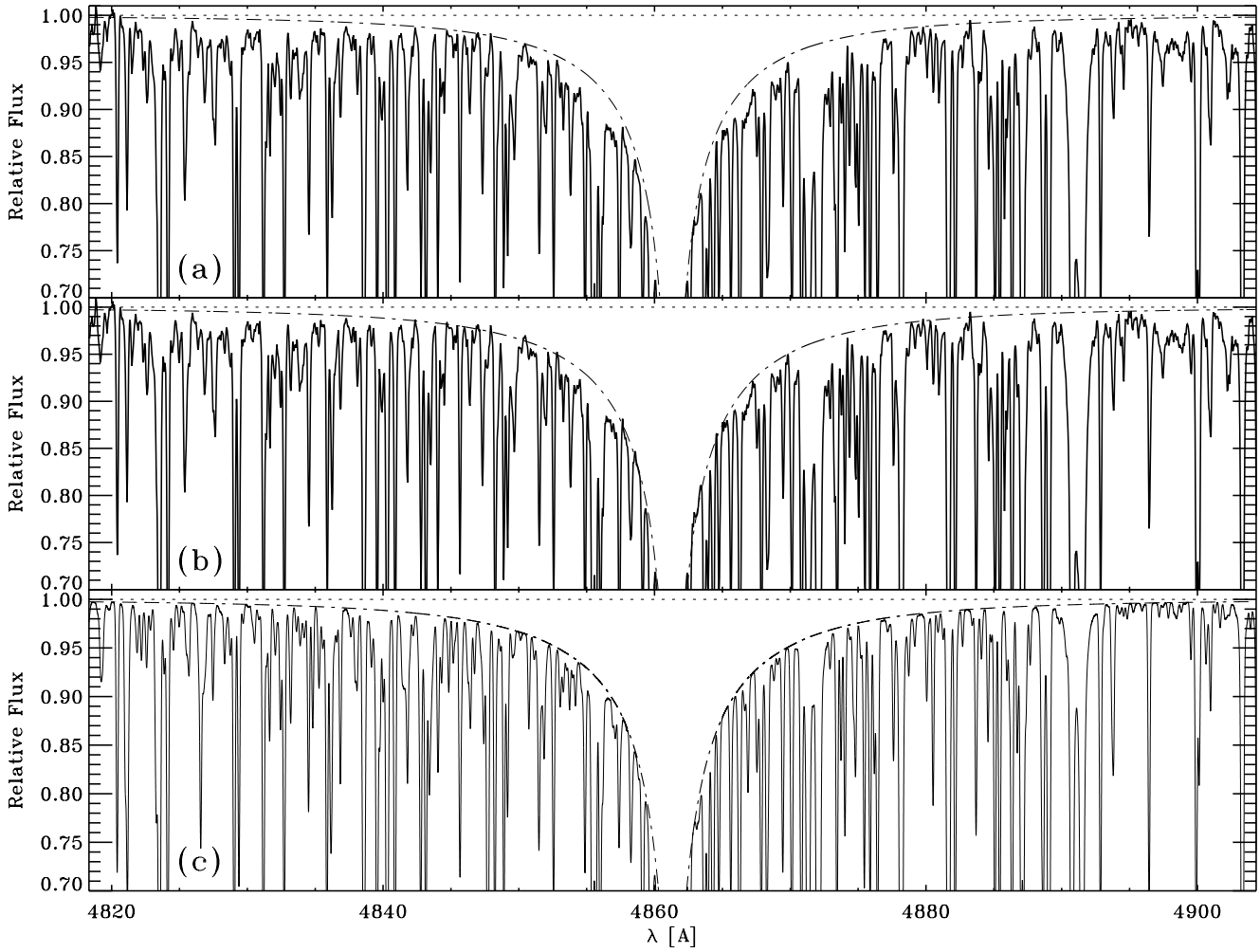

Fig. 6. Same as Fig. 5, but for Hβ, which is superposed by strong line-blanketing. Bottom panel: spectrum synthesis of ∼3100 unadjusted, but convolved atomic + molecular lines. As in Fig. 5, the comparison of panels (b) and (c) shows that tracing the Balmer line wings from the "high points" in panel (b) is feasible at the resolution of the FOCES spectrograph

ever, are small and not taken into account. Table 2 summarizes the atomic data of the Mg I lines employed in the analyses.

Table 2. Line data of Mg I lines

λ [Å]	χ_{low} [eV]	$\log gf$	$\log C_6$	$\log C_4$	γ_{rad} [$10^8 s^{-1}$]
4571.097	0.00	–5.59	–31.20	-	0.000
4730.031	4.33	–2.34	–28.80	-	4.768
5172.697	2.70	–0.39	–30.88	–14.52	1.002
5183.616	2.70	–0.17	–30.88	–14.52	1.002
5528.415	4.33	–0.50	–30.43	–13.12	4.908
5711.093	4.33	–1.70	–30.00	-	4.817

4. The stellar parameters of Procyon

From a rather conservative point of view one may state that only the Sun provides well-defined parameters in the regime of dwarf F and G stars. There is, however, recent progress in stellar diameter measurements which confirms the results of Hanbury Brown et al. (1974) who determined Procyon's angular diameter to be 5.50 ± 0.17 mas from intensity interferometry. The new Mark III Optical Interferometer measurements of Mozurkewich et al. (1991) yield the same value 5.508 ± 0.050 mas, but with a considerably reduced error. With this angular diameter measurements the most *direct* methods to determine the effective temperature result in (cf. Steffen 1985)

(a) $T_{eff} = 6561 \pm 166K$

(b) $T_{eff} = 6516 \pm 103K$

if we make use of (a) the bolometric magnitudes from Code et al. (1976), or (b) the measurement of the in-

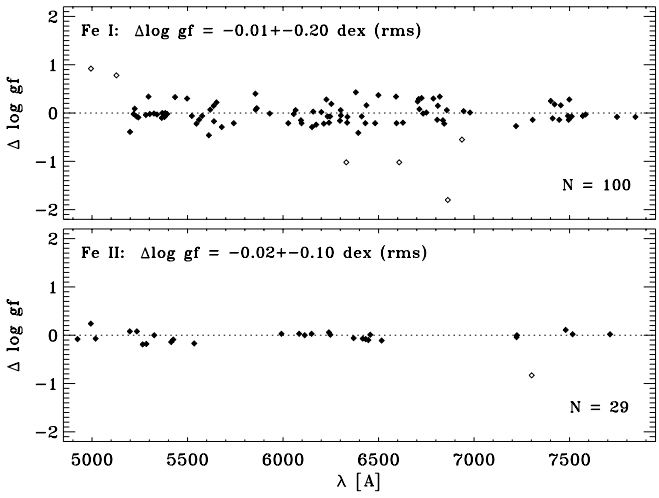

Fig. 7. Comparison of astrophysical versus theoretical (Kurucz 1992a) iron oscillator strengths. Top: Fe I, bottom: Fe II. There is no systematic difference $\Delta \log gf$ (Kurucz – this work) if we discard the few mavericks indicated by open symbols. The solar abundance assumed in deriving the astrophysical gf-values is the meteoritic value $\log \epsilon(\mathrm{Fe}) = 7.51$

tegrated flux. In the latter case we take the average from Code et. al. (1976): 18.08±0.76, Beeckmans (1977): 18.14±1.14, Blackwell & Shallis (1977): 18.0±0.8 and Smalley & Dworetsky (1995): 18.638±0.868 (in units of 10^{-6} erg· cm^{-2}· s^{-1}) with an estimated uncertainty of $0.8 \cdot 10^{-6}$ erg· cm^{-2}· s^{-1}. Hence we get a mean value for the effective temperature

$$\boxed{T_{eff} = 6530 \pm 90K}$$

While this is already a relatively small error for stellar abundance analyses, Procyon – being a visual binary ($P \sim$ 40 years, $a \sim 16$ AU) – supplies a very precise value for the surface gravity, too. According to $g = GM/R^2$ we need to know the stellar mass and radius. The latter is obtained from the above mentioned angular diameter in combination with the stellar distance. Irwin et al. (1992) derive an absolute parallax of $\pi = 0.2899 \pm 0.0074$ arcsec and compare this to the recent value published by the U. S. Naval Observatory $\pi = 0.2864 \pm 0.0023$ arcsec (cited by Irwin et al.). Along with the data from Mozurkewich et al. (1991), Procyon's radius is then found to be $R = 2.04 \pm 0.07 R_\odot$ and $R = 2.07 \pm 0.03 R_\odot$, respectively.

From the orbital parameters of Procyon and its white dwarf companion Irwin et al. also supply a value for the stellar mass with $1.69 \pm 0.13 M_\odot$ or $1.751 \pm 0.051 M_\odot$, depending on whether they use (a) their own parallax value or (b) the one proposed by USNO, and therefore

(a) $\log g = 4.05 \pm 0.06$

(b) $\log g = 4.05 \pm 0.02$

i.e. one may adopt

$$\boxed{\log g = 4.05 \pm 0.04}$$

although an error even twice as much could be entitled "very precise" in the context of stellar atmosphere analyses.

One has, however, to concede that from the stellar evolutionary point of view Procyon is too massive by $\sim 0.3 M_\odot$. But this well-known discrepancy (cf. Steffen 1985, Irwin et al. 1992, and references therein) can be solved if – as Irwin et al. suggest – the separation of the binary components has been systematically overestimated by approximately 0.2 arcsec. Irwin et al. point out that observations of this kind are extremely difficult since the magnitude difference of the primary and secondary in the Procyon system is quite large ($\Delta V = 10$). It is also worth mentioning that their analysis with respect to the visual binary separation is based on Lick and Yerkes data from 1897 to 1913. For this reason they suggest that a modern observational study of the Procyon separation should be initiated to remove this uncertainty and further studies are obviously underway (cf. Dyson et al. 1994, Walker et al. 1994), or will profit from the availability of the HIPPARCOS catalogue in 1997.

For the time being, if one simply adopts a mass of $M = 1.45 M_\odot$ the surface gravity is changed to $\log g = 3.97$, but this inevitably means that the $\log g$ parameter does not benefit very much from the precise knowledge of the stellar mass.

At this stage, having established Procyon's effective temperature and surface gravity by very direct methods, we turn to the iron abundance and model atmosphere analyses. Let us first briefly recall the problem Steffen demonstrated ten years ago: in his analysis of the Procyon spectrum of Griffin & Griffin (1979) an ATLAS6 model atmosphere (Kurucz 1979) with $T_{eff} = 6500$ K and $\log g = 4.04$ produced inconsistent abundances from lines of neutral and ionized stages of the same element. Abundances derived from ionized lines are systematically higher than those resulting from neutral lines in all cases where both kinds of lines are available. Steffen is able to reconcile this dichotomy by increasing the effective temperature to 6750 K, but favours 6500 K to be the most probable value, albeit the ionization equilibrium calls for an unrealistic $\log g \approx 3.55$ in this case. Instead of looking for compromises by taking some kind of "mean values" as others did before and later, Steffen *emphasizes* this discrepancy and suggests NLTE effects and temperature inhomogeneities associated with convective motions (cf. Gray 1981b, Dravins 1987) as possible explanations. But irrespective of these problems he also points out that abundances derived from lines of nearly completely ionized elements (like Mg II, Si II, Fe II...) are quite *insensitive* to NLTE effects, the effective temperature and uncertainties

in the temperature structure. Consequently, lines of this kind are most reliable for abundance analyses in our temperature range *provided the value for the surface gravity is known.*

Contrary to the analysis of Steffen, who had to work with photographic material obtained during several years, our data are CCD-based and homogeneous due to the large wavelength range achieved with one exposure. Therefore, as a first step, it was reassuring that our analysis gave the same results as Steffen's to within the error bars (cf. Fig. 8 and 9). The model atmosphere we use for Procyon is similar to Steffen's ATLAS6 model, except for that we use $\alpha = 0.5$ for the mixing-length in the convective energy transport. The wings of the Balmer lines Hα and Hβ indicate the effective temperature $T_{eff} = 6470$ K. With this value and taking Fe II lines and high-excitation ($\chi_{low} > 4$ eV) Fe I lines into account, the ionization equilibrium provides $\log g = 3.58$, a microturbulence value $\xi_t = 1.95$ km s^{-1} (in the usual manner that lines of different strength should give the same abundance) and a metal abundance [Fe/H]$= -0.10$.

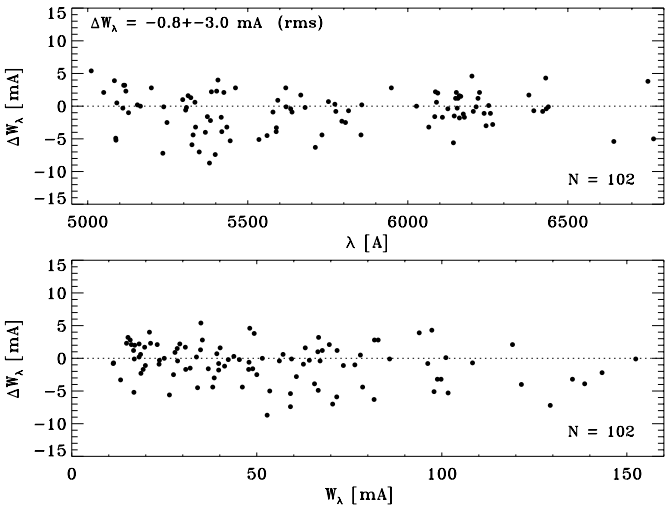

Fig. 8. Equivalent width measurements in the FOCES spectrum of Procyon compared to those of Steffen (1985). The mean difference in the sense ΔW_λ (this work – Steffen) is -0.8 mÅ

Note that the value for the effective temperature is 30 K beneath the one of our previous analysis (Fuhrmann et al. 1993) which was based on Kurucz (1979) opacities. This is however analogous to the Sun, where the wings of the Balmer lines indicate 5750 K, as has been discussed in Sect. 3. If we would instead adopt a value of 6530 K the ionization equilibrium would still be very discrepant with $\log g = 3.65$. To reconcile the surface gravity value with the astrometric one, we have to increase the effective temperature to $\sim$ 6800 K (cf. Fig. 9), which is of course beyond a reasonable limit.

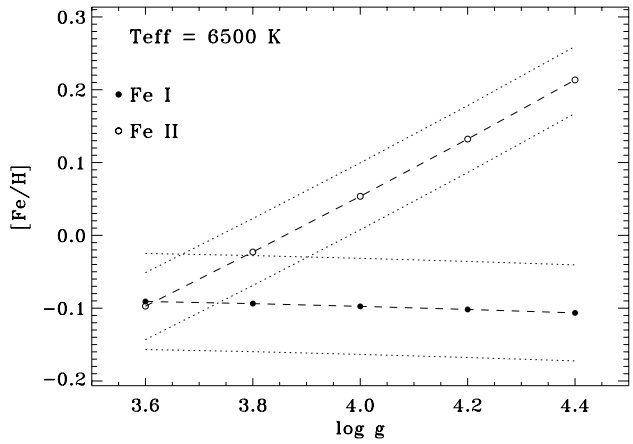

Fig. 9. The ionization equilibrium of iron in the model atmosphere analysis of Procyon with $T_{eff} = 6500$ K. Dashed lines indicate the abundances of Fe I (filled circles) and Fe II (open circles) as a function of surface gravity. The dotted curves are the 1σ error bars (rms) valid at $\log g \sim 3.62$, the intersection of Fe I and Fe II abundances. Lines of neutral iron depend on the precise value of the effective temperature with Δ[Fe/H]~ 0.06 dex for a change of $\Delta T_{eff} = 100$ K. Fe II instead is very sensitive to the surface gravity parameter, but almost independent to a change in the effective temperature (Δ[Fe/H]< 0.01 dex for $\Delta T_{eff} = 200$ K). The discrepancy at $\log g = 4.05$, the astrometric surface gravity of Procyon, amounts Δ[Fe/H]$= 0.17$ dex. To reconcile the Fe I and Fe II abundances an unrealistic high effective temperature of $\sim$ 6800 K would be required

As a consequence, this inevitably means that our standard model atmosphere analysis is restricted by severe limitations in the ionization equilibrium. Because neutral iron exists to merely about $\sim$1% in the line forming regions of Procyon, it is very susceptible to details in the temperature structure. Small turbulent motions capable to produce temperature inhomogeneities or deviations from the Saha-Boltzmann population numbers obviously have their impact on the line formation process and there is evidence that especially NLTE effects are at work (Watanabe & Steenbock 1985).

In this situation it is natural to ask whether we can postpone these difficulties and follow instead another, more trustworthy path to derive the surface gravity parameter. This in fact seems possible from the analysis of strong lines, as proposed in what follows.

As a rule, it is known that stars like Procyon which possess an extreme ionization balance in e.g. Fe I/Fe II or Mg I/Mg II, have the opposite advantage of being almost insensitive to pressure changes in the line formation of *weak neutral lines*. That is, provided one can find a scarcely populated species, which nevertheless forms weak *and* strong lines in the same stellar spectrum, the determination of the surface gravity value can be achieved.

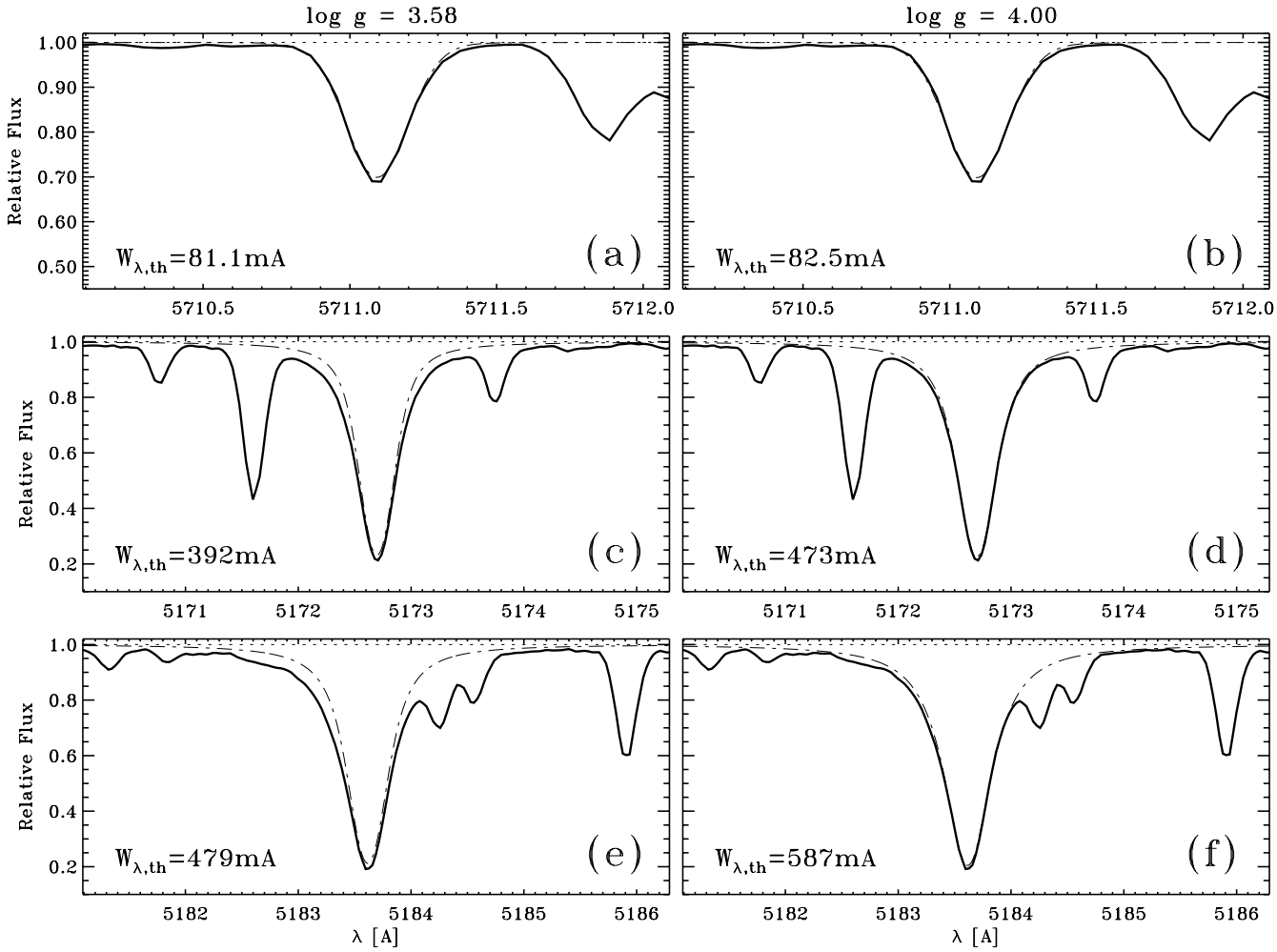

Fig. 10. The spectroscopic surface gravity determination of Procyon from the analysis of Mg I lines. Left column: line profiles of Mg I λ5711 (top) and the Mg Ib lines λ5172 and λ5183 (below) for a surface gravity value $\log g = 3.58$, as derived from the ionization equilibrium. The profile of λ5711 shows no wings and is practically independent of the surface gravity, as illustrated in panel (b), where line formation is done for a value $\log g = 4.00$. Among other weak Mg I lines, λ5711 therefore serves to fix the value of the Mg I abundance. This information is *then* used in the analysis of λ5172 and λ5183 by altering the surface gravity value until the observed line shape is reproduced as shown in panels (d) and (f). In the case of Procyon $\log g = 4.00$ is found by this method, which is 0.42 dex higher than derived from the ionization equilibrium and only slightly below $\log g = 4.05$, the very precisely known value from astrometric data

In this respect we advocate Mg I to be a good tracer of the surface gravity parameter, because

(a) the oscillator strengths, especially the ones of the Mg Ib lines are fairly well-known, consequently it is a straightforward task to derive the collisional damping constant from the line shape in the solar flux spectrum
(b) the Mg Ib lines lie in a spectral region where an accurate (0.5 - 1%) placement of the continuum is feasible
(c) although λ5167 is heavily blended, redundancy in the measurements is achieved from λ5172 and λ5183
(d) magnesium has approximately the same ionization potential and cosmic abundance as iron. Hence it is one of the most abundant elements, and – in our temperature range – the neutral stage is much less populated than the ionized one, i.e. weak neutral lines become insensitive to the surface gravity parameter
(e) the strong Mg Ib lines show wings even in metal-poor stars of [Fe/H]< -2, which is most important for our stellar sample (e.g. HD 19445)

In Figure 10 we apply the information stored in the Mg I lines to the spectrum of Procyon: in the left column λ5711 and the Mg Ib lines λ5172 and λ5183 are shown for the surface gravity value $\log g$=3.58 as derived from the ionization equilibrium. λ5711 is practically an unblended absorption line and – as is obvious from panel (b) – insensitive to a change in $\log g$ from 3.58 to 4.00 ($\Delta W_\lambda = 1.4$ mÅ). The theoretical profiles (dashed lines) have been convolved with a rotational broadening compo-

nent $v\sin i = 2.8 \pm 0.3$ km s^{-1}, a radial-tangential macroturbulence $\zeta_{RT} = 7.0 \pm 0.1$ km s^{-1} (both adopted from Gray 1981a) and the instrumental profile (a Gaussian of 4.6 ± 0.2 km s^{-1}). The final profile fit to λ5711 in panel (a) is now achieved by simply adjusting the magnesium abundance. Once we have fixed the Mg I abundance from this and other weak Mg I lines, it serves as the input parameter to the Mg Ib lines. They possess strong wings and respond to a change in $\log g$, as shown in panels (d) and (f). It is important to realize that the magnesium abundance derived from weak Mg I lines has *no* meaning in an absolute sense. It merely serves as the input parameter to the strong Mg Ib lines, which makes this differential procedure a very robust one. If instead, we would have done the whole analysis with $T_{eff} = 6530$ K, i.e. a 60 K higher value, the surface gravity would result in $\log g = 4.02$.

In practice the method is of course iterative. In the case of Procyon it takes two iterations to obtain the final parameters. In the first step we get $\log g \sim 3.90$ from the profile fit to λ5172 and λ5183 and derive a new value for the microturbulence and iron abundance (e.g. [Fe/H] is increased from $= -0.10$ to -0.02). In addition, these two parameters are now derived exclusively from Fe II lines to make sure that the LTE assumption is fulfilled and to be independent of details in the temperature structure and effective temperature value. After a slight reiteration of the effective temperature from Balmer lines the next step already provides the final spectroscopic parameters:

$$T_{eff} = 6470 \text{ K}$$
$$\log g = 4.00$$
$$[\text{Fe/H}] = +0.01$$
$$\xi_t = 2.09 \text{ km s}^{-1}$$

Note, as explained above, the effective temperature turns out to be somewhat low compared to the direct methods from the angular diameter measurements, but this has practically *no* influence on the other three parameters, that is, irrespective of small uncertainties in the effective temperature value it seems possible to find very reliable parameters for the surface gravity, the iron abundance and the microturbulence. Reasonable error limits in the case of Procyon are $\Delta \log g = 0.1$ dex, Δ[Fe/H]= 0.07 dex and $\Delta\xi_t = 0.3$ km s^{-1}.

5. Application to other F and G stars

In a next step, we now apply the strong line method to other stars of the same temperature/gravity range and compare the stellar parameters to the ones we would obtain from the ionization equilibrium.

As in the case with Procyon, we first need to know both, the rotational and macroturbulence velocities for subsequent line profile analyses. To a very good approximation we treat all stars of our sample as slow rotators. This especially holds true for the metal-poor stars, which may be as old as or even older than the Galactic disk. In addition the instrumental profile (a Gaussian of 4.6 ± 0.2 km s^{-1}) acts as the dominant contributor to the convolution profile for most objects of our sample. Therefore elaborate Fourier techniques are not considered here. Instead we make reasonable assumptions with respect to the rotational velocities (e.g. $v\sin i = 1$ km s^{-1} for HD 19445 and HD 140283) and, along with the known instrumental profile, deduce the macroturbulence from the observed line shape. Note also that $v\sin i$ and ζ_{RT} do compensate each other to some extent. A star that actually rotates some 3 - 4 km s^{-1} faster than assumed, will merely receive a higher macroturbulence parameter, whereas the other stellar parameters are practically unchanged. As has been suggested from time to time there are also observational hints that the values adopted for micro- and macroturbulence are correlated; thus, knowing the microturbulence parameter, one can estimate the macroturbulence to a first approximation. For the Sun we have $\zeta_{RT}/\xi_t = 3.5/0.9 \sim 3.9$, whereas Procyon shows a ratio of $\zeta_{RT}/\xi_t = 7.0/2.1 \sim 3.3$. All other objects in Table 3 roughly fit to this assumption, with ~ 2.3 and ~ 4.3 as lower and upper limits.

A very important test for the accuracy of our analyses and the performance of the spectrograph is the investigation of the Moon spectrum from the reflected sunlight. For this purpose, three short exposures were obtained and added to a combined spectrum. The Kitt Peak Solar Flux Atlas degraded by a Gaussian of 4.6 ± 0.2 km s^{-1} shows the great similarity of both spectra (cf. Fig. 3). Comparing the equivalent widths of iron lines one obtains $\Delta W_\lambda(Moon - KittPeak) \sim 0.5$ mÅ, with an 1 σ rms error of ~ 1.8 mÅ. Due to the somewhat lower effective temperature (cf. Fig. 5 and 6), log g is changed as well, if derived from the ionization equilibrium; the strong line method, on the other hand, results in the solar value log $g = 4.44$ (cf. Table 3, Fig. 11). The iron abundance derived from 9 Fe II lines is found to be slightly too high by 0.05 dex, which reflects the uncertainties from the strong line blanketing in the solar spectrum. This tendency may also be present in the spectra of Procyon and o Aquilae, but is negligible in the metal-poor stars. Nevertheless, the analysis shows that, to within the error bars, the parameters derived from the Moon spectrum, reproduce the actual solar values.

In analogy to the analysis of Procyon, Fig. 12 displays the surface gravity determination of HR 1545, a metal-poor star 200 K cooler than Procyon. The discrepancy of the iron ionization equilibrium vs. the strong line method amounts to 0.22 dex and, again, leads to a *higher* log g. Table 3 indicates that this star is also enriched in the α-element magnesium by [Mg/Fe]=+0.14 dex. We therefore repeated the analysis on a grid of model atmospheres with α-elements enhanced by +0.4 dex. As a result, the iron

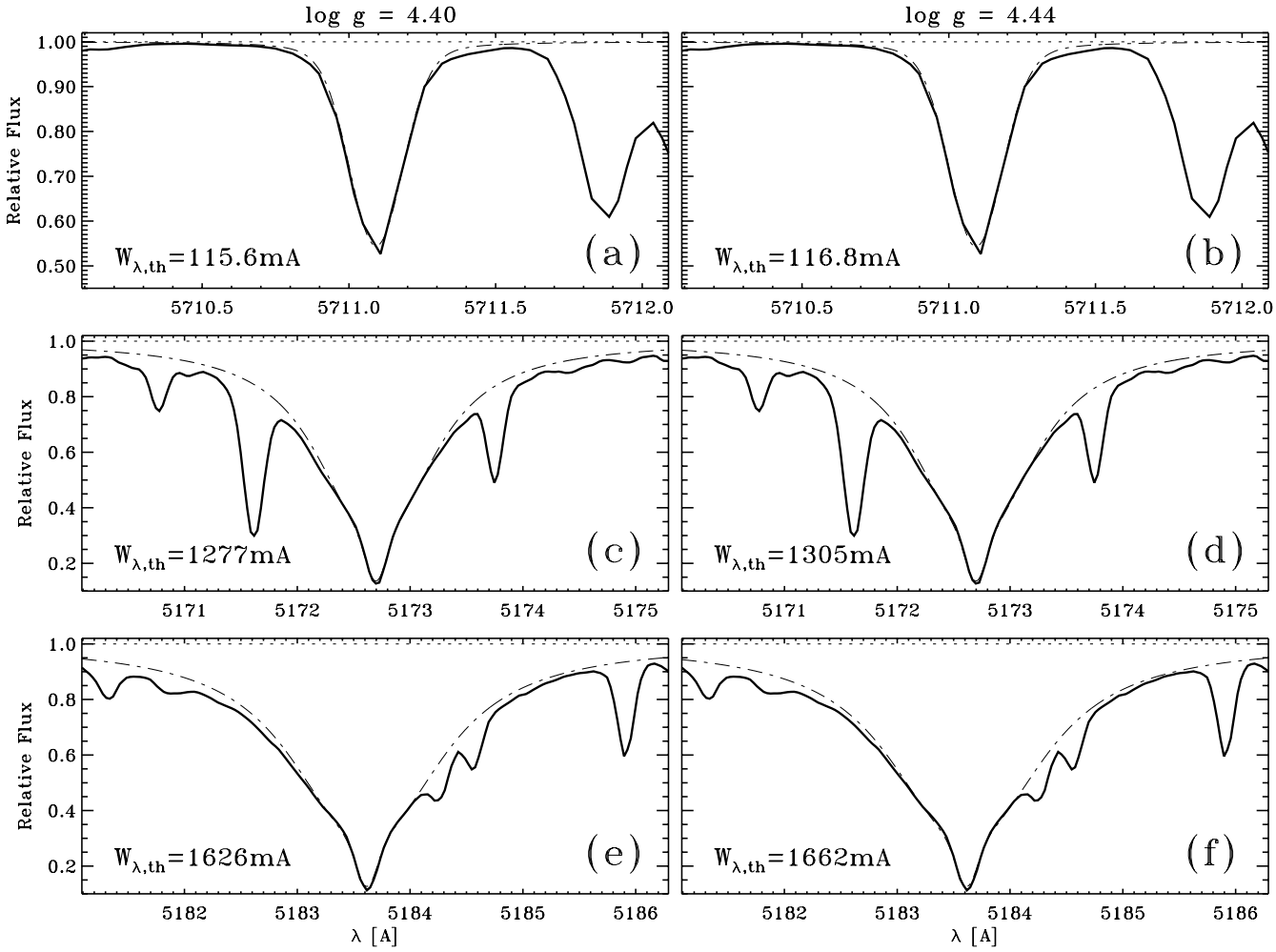

Fig. 11. The spectroscopic surface gravity determination of the Moon (= reflected sunlight) spectrum (cf. Fig. 10). Left column: $\log g = 4.40$ derived from the ionization equilibrium. Right column: $\log g = 4.44$ from the analysis of Mg I lines

Table 3. Stellar parameters derived from Balmer lines (T_{eff}), the strong line method ($\log g$) and singly ionized iron lines ([Fe/H], ξ_t). For comparison purposes, the surface gravity and iron abundance deduced from the ionization equilibrium (I.E.) of Fe I/Fe II are listed in columns (8) and (9), with the number of Fe I and Fe II lines used in columns (10) and (11). The values in column (5) and (6) are, however, based on Fe II lines only. For all Fe I lines $\chi_{low} > 2$ eV is taken as a lower limit, except for Procyon, where $\chi_{low} > 4$ eV is adopted. The Moon spectrum (bottom row) – treated as a *star* – serves for comparison and to obtain the instrumental profile, which is found to be a Gaussian of 4.6 ± 0.2 km s^{-1}. Rotational and macroturbulence velocities for the line profile analyses are given in columns (12) and (13). The last column indicates, whether models with scaled-solar abundances ($\odot$), or α-elements enhanced by +0.4 dex (α) were employed. For HR 1545 both results are shown

(1) Object	(2) HD	(3) T_{eff} [K]	(4) $\log g$	(5) [Fe/H]	(6) ξ_t [km/s]	(7) [Mg I/Fe I]	(8) $\log g$ (I.E.)	(9) [Fe/H] (I.E.)	(10) Fe I	(11) Fe II	(12) $v \sin i$ [km/s]	(13) ζ_{RT} [km/s]	(14) Instr. [km/s]	(15) M
HR 17	HD 400	6156	4.07	−0.26	1.38	+0.08	(3.98)	(−0.36)	(29)	10	4.2	5.9	4.6	$\odot$
	HD 19445	6040	4.36	−1.97	1.32	+0.48	(4.12)	(−2.08)	(16)	3	1.0	3.0	4.6	α
HR 1545	HD 30743	6288	4.02	−0.48	1.60	+0.14	(3.80)	(−0.57)	(24)	10	5.5	5.6	4.6	$\odot$
"	"	6295	4.10	−0.42	1.61	+0.16	(3.73)	(−0.57)	(24)	10	5.5	5.6	4.6	α
HR 2943	HD 61421	6470	4.00	+0.01	2.09	+0.02	(3.58)	(−0.10)	(11)	7	2.8	7.0	4.6	$\odot$
	HD 140283	5843	3.52	−2.34	1.48	+0.32	(3.20)	(−2.47)	(10)	4	1.0	5.3	4.6	α
HR 7560	HD 187691	6074	4.08	+0.08	1.29	+0.02	(4.06)	(+0.07)	(30)	8	3.0	4.5	4.6	$\odot$
	HD 194598	6050	4.27	−1.11	1.31	+0.28	(4.19)	(−1.16)	(24)	8	2.0	4.2	4.6	α
	HD 201891	5948	4.19	−1.05	1.15	+0.38	(4.14)	(−1.10)	(23)	7	2.0	4.0	4.6	α
Moon		5753	4.44	+0.05	0.82	−0.02	(4.40)	(+0.02)	(19)	9	1.7	3.5	4.6	$\odot$

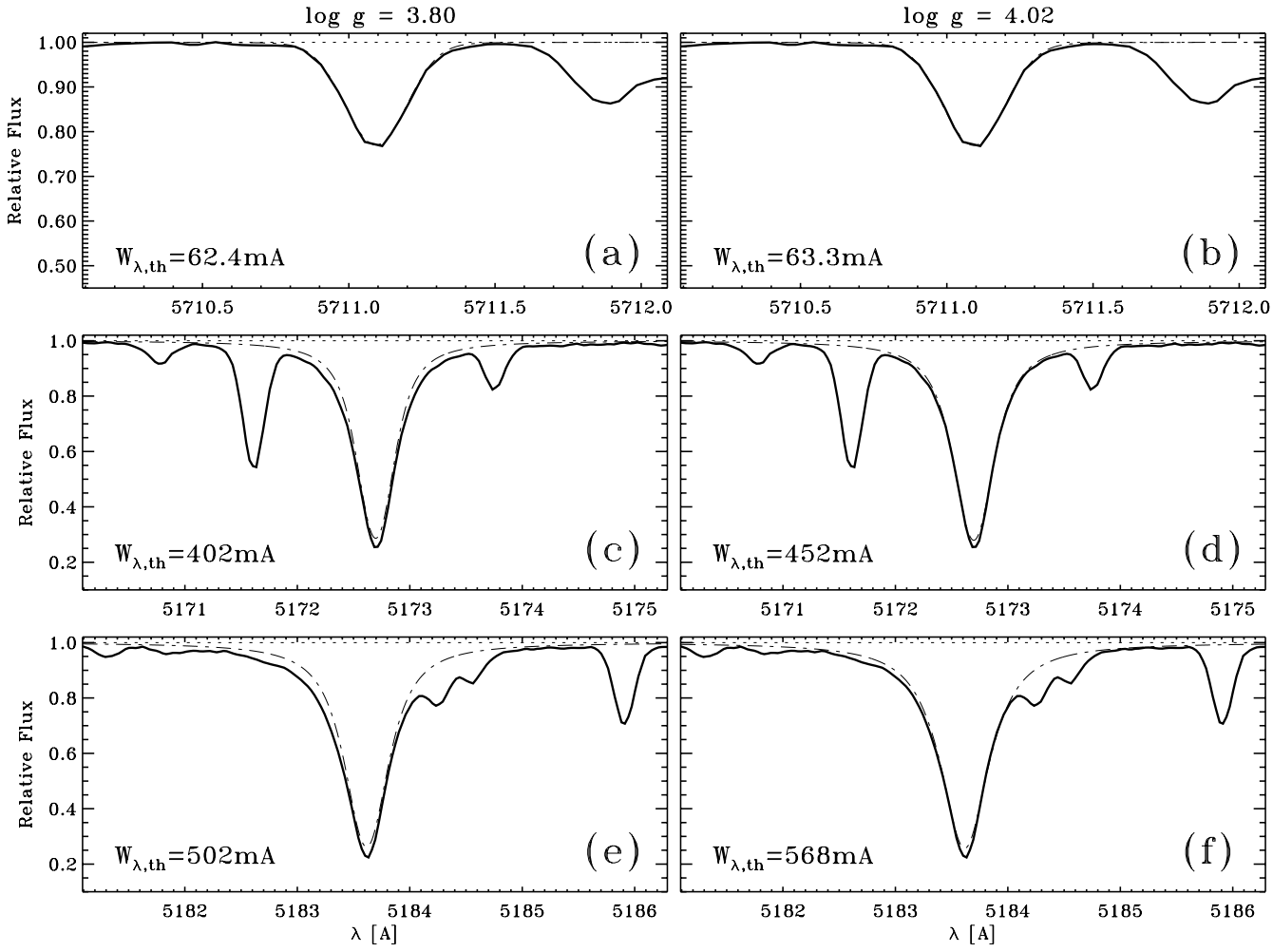

Fig. 12. The spectroscopic surface gravity determination of HR 1545 (cf. Fig. 10). Left column: $\log g = 3.80$ derived from the ionization equilibrium. Right column: $\log g = 4.02$ from the analysis of Mg I lines

abundance is changed from –0.48 to –0.42 and the surface gravity increases to log $g = 4.10$. Hence the final parameters for this star should be obtained from interpolation within these two limiting cases.

HD 19445, in Fig. 13, is one of the standard halo stars, whose radial velocity and spectral appearance was found to be peculiar as early as 1914 by Adams & Kohlschütter. Later Chamberlain & Aller (1951) demonstrated that this star is underabundant in metals. Since then many analyses have been published on this object, not always without contradicting results. Our investigation of the ionization equilibrium shows a log $g = 4.12$ and an iron abundance [Fe/H]= −2.08. The surface gravity derived from the Mg Ib lines increases this value to log $g = 4.36$, whereas the iron abundance changes by ~ 0.1 dex to [Fe/H]= −1.97. This value, as well as the microturbulence $\xi_t = 1.32$ km s^{-1}, is however based on only three Fe II lines. On the other hand, repeating the analysis with Fe I lines only, would result in [Fe I/H]= −1.99 and $\xi_{t,\mathrm{Fe\ I}} = 1.46$ km s^{-1}. Our analysis therefore puts this object closer to the main sequence, whereas the value of the ionization equilibrium suggests a turnoff stage. Implications following these findings will be addressed in the final section. Note especially, that both Mg Ib lines are still strong enough to show pronounced wings, although HD 19445 is depleted in iron by a factor of 100. The same holds true for HD 140283, with $W_{\lambda 5172} \sim 146$ mÅ and $W_{\lambda 5183} \sim 168$ mÅ, for which we obtain similar systematics. Both halo stars reveal however considerable deficiencies in the line cores of λ5172 and λ5183 which may restrict the applicability of our LTE analysis.

Closer inspection of Table 3 indicates that all stars receive higher log g values with the strong line method. The discrepancy is strongest for Procyon, the hottest star in our sample, and gets smaller the closer we come to the solar parameters, as expected for a differential analysis. HD 140283, for instance, is only slightly hotter than the Sun, but its evolved stage and metal-deficiency shifts this star to a region where the ionization balance is comparable to that of Procyon.

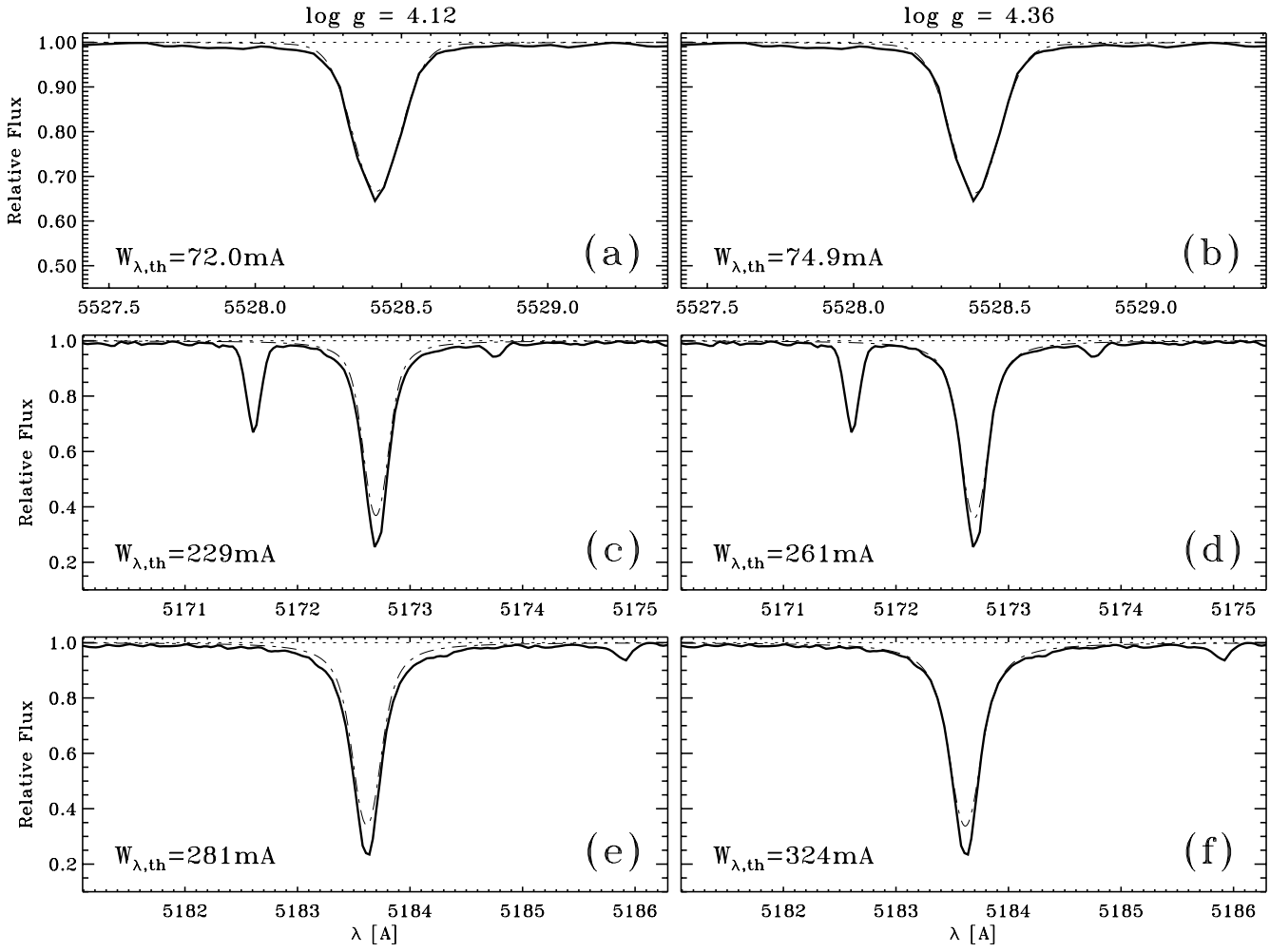

Fig. 13. The spectroscopic surface gravity determination of HD 19445 (cf. Fig. 10). Left column: $\log g = 4.12$ derived from the ionization equilibrium. Right column: $\log g = 4.36$ from the analysis of Mg I lines. Note in panel (a) and (b) λ5528 is used instead of λ5711, which is rather weak ($\sim$10 mÅ) in HD 19445

As a second result of Table 3 we mention a slightly increased metal abundance scale by $\sim +0.1$ dex on average. Individual Fe I and Fe II abundances can however deviate by up to 0.2 dex. This is not immediately obvious from Table 3, where column (9) gives the mean abundance of neutral *and* ionized lines. Column (5) instead results from Fe II lines only, a different $\log g$ and different ξ_t. The analysis of Procyon, e.g. leads to [Fe I/H]=−0.16 and [Fe II/H]=+0.01 for $\log g = 4.00$.

Reasonable error bars for the analyzed stars are similar to the ones mentioned for Procyon. The effective temperature can be fixed to $\sim$ 80 K from a single Balmer line. With both, Hα and Hβ, as well as redundant spectra, errors in the placement of the continuum can be estimated, and a formal error well below 50 K is achieved. On the other hand, the wings of the Balmer lines are the result of a temperature structure which in turn depends on the convective efficiency and the line blanketing. To assess the reliability of the Balmer line method we refer to the Sun and Procyon, where a small systematic effect (cf. Fig. 5 and 6) is indicated, at least for metal-rich stars. All other stars are based on the same kind of model atmosphere and show consistent results for all Balmer lines. We therefore estimate the *true* effective temperatures to be most probably within 100 K of the values given in column (3) of Table 3.

The determination of the surface gravity is not very much affected by the exact value of the effective temperature. From direct inspection of the pressure-broadened profiles of the Mg Ib lines, accuracies on the 0.05 dex scale can be achieved without doubt and redundancy is obtained from λ5172, λ5183 and repeated observations. The strong line method depends however on the adopted magnesium abundance value, which in turn is fixed from weak Mg I lines and brings velocity and turbulence parameters as well as the instrumental profile into play. Again, we estimate the resulting accuracies in combination with the individual data for the Sun and Procyon. Taking all uncer-

tainties into account, an error less than $\Delta \log\ g \sim 0.1$ dex is expected.

Finally the iron abundance derived from Fe II lines is insensitive to a precise knowledge of the effective temperature, the temperature structure and NLTE effects. On the contrary, it depends on the surface gravity and, due to the paucity of useful Fe II lines (especially in metal-poor stars), on the microturbulence parameter. We estimate the Fe II abundance determinations to be better than 0.1 dex, but consider the microturbulence values to be erroneous by 0.2 to 0.3 km s^{-1}.

6. Discussion and conclusions

The data we presented in the preceding sections benefit very much from the recently installed fiber optics cassegrain échelle spectrograph FOCES: the effective temperatures of the stellar objects are determined from the *simultaneous* observation of Hα λ6562 and Hβ λ4861, supplemented by Hγ λ4340 and Hδ λ4101 in metal-poor stars. The gravity determination employs lines, such as Mg I λ4571 and Mg I λ5711, which are separated by more than 1000 Å, but homogeneous in the data reduction. The abundance analysis is confined to iron lines as free of blends as possible. Again, a range spanning about 2000 Å is considered for this purpose.

First light for this spectrograph has been a solar spectrum, which we compared to the Kitt Peak Solar Flux Atlas (Fig. 3) and which was subsequently used to derive the "stellar parameters" of the Sun. These initial tests were then followed by a detailed investigation of the notorious F5 standard Procyon. Similar to the results of Steffen (1985), a log g around 3.6 is obtained from the ionization equilibrium of iron lines, in sharp contrast to the accurately known astrometric value log g = 4.05. This discrepancy is however circumvented if we employ the wings of the strong Mg Ib lines. The analysis of other cool dwarf stars in this temperature range shows similar, albeit less pronounced, systematic deviations in the gravity determination. In this respect our results completely agree with the findings of Edvardsson (1988b), although our objects are about $\sim$ 1000 K hotter on average.

There is, however, a number of uncertainties we have to be aware of. First of all, we learn from the analysis of the Procyon spectrum, that the standard model atmosphere approach has severe limitations. NLTE effects may be responsible in the case of Procyon, as well as other, especially metal-poor stars (e.g. Magain & Zhao 1996). The underlying temperature structures pose additional questions. Here, the treatment of convection and the amount of line blanketing – to name only two of the ingredients – deserve special attention. Obviously none of contemporary model atmosphere programs can reproduce *all* observable parameters such as the continuous energy distribution, the limb darkening or Balmer line formation (cf. Holweger et al. 1995, Castelli et al. 1996). Since our approach is to derive the stellar parameters exclusively from the analysis of spectral lines, we give most weight to the information available from these tracers. This has led to the empirical calibration of the mixing-length parameter from the analysis of Balmer lines in Fuhrmann et al. (1993). The value proposed in that work, $\alpha = 0.5$, is still the one we prefer in our actual grid of model atmospheres (the exact number, of course, depends on which formalism of the mixing-length theory one refers to, and the kind of model atmosphere program used).

But can we trust such empirical calibrations? How reliable are the so-derived stellar parameters? We have argued in the sections above, that accurate stellar parameters from very direct methods in our temperature/gravity range are only known for Procyon. From the wings of its Balmer lines we find an effective temperature close to the interferometric value. The analysis of Fe I lines reveals shortcomings in the ionization equilibrium, but the very differential method to derive the gravity parameter from the strong Mg Ib lines sticks close to the astrometric value. It seems very unlikely that these results are fortuitous.

In their analysis of Arcturus Blackwell & Willis (1977) considered the Mg Ib line λ5172 to be unsuitable for a surface gravity determination, because of a lack of weak lines for the abundance determination originating from a similar lower level. In addition, Edvardsson (1988b) argued that the Mg Ib lines are notably asymmetric, which led him to exclude the triplet from his list of appropriate strong lines.

Inspection of Fig. 10 and 11 shows especially λ5183 to be slightly asymmetric on the short-wavelength side, but this does not influence our results very much. Excluding the line core of λ5183 from the analysis, a slight shift of the observed profile to longer wavelengths is feasible. As a consequence the surface gravity value can be increased to match the observed profile. The correction is however very small and, in the case of Procyon, adjusts the log g value from 4.00 to 4.02 only. For this reason we do not carry out a detailed synthetic spectrum analysis of the $\lambda\lambda 5160 - 5190$ region. Instead our approach in Fig. 10 to 13 is rather conservative in that we increase the log g until at least *one* wing matches the observations. The proposed log g values are therefore lower limits on the $\sim$ 0.02 dex scale if line blends play a role, whereas metal-poor stars remain unaffected and show symmetrical wings (cf. Fig. 13).

The absence of suitable weak magnesium lines from $\chi_{low} = 2.7$ eV, the lower level of the Mg Ib lines, is certainly disadvantageous to our analysis. Erroneous effective temperatures, as well as NLTE effects may have some impact on the results. It is therefore encouraging that the two most important Mg I lines we make use of, λ4571 ($\chi_{low} = 0.0$ eV) and λ5711 ($\chi_{low} = 4.3$ eV) are consistent in the magnesium abundance to within 0.03 dex for each star (HD 19445 and HD 140283 are excluded, since both lines are rather weak in these stars). We take this as

further evidence that our temperature scale is adequate and the surface gravities reliable to 0.1 dex. It is only for the very metal-poor stars that the uncertainties increase, because less absorption lines of iron and magnesium are available and the Mg Ib lines show larger deviations in the line cores (cf. Fig. 13).

The systematic deviation of the surface gravity parameters in Table 3 has of course consequences on the kinematics and evolution of the Galaxy. HD 19445, for instance, is either close to the main sequence or in the region of turnoff stars depending on which surface gravity determination we refer to. With the larger $\log g$ parameter all stars become less distant and consequently the space velocities decrease. Another direct implication arises from the comparison of evolutionary sequences, where considerable changes of the stellar ages are conceivable.

Due to our differential analysis, we do not expect large deviations in the stellar parameters for stars that are close to the Sun in neither $\log g$ nor the metal abundance. For cooler objects notable changes may arise, but certainly the hotter stars with their extreme ionization balance of iron and magnesium are prone to considerable changes if we dismiss the ionization equilibrium and especially Fe I lines from the analysis of stellar parameters of F and G stars.

In conclusion, the bright F5 star Procyon is an encouraging example to demonstrate that reliable stellar parameters for this object can be derived from conventional model atmosphere analyses. Nevertheless, the situation is unfortunate in that we have no other calibrating stars at our disposal in the temperature/gravity range considered here. In this respect, the most urgent task is to improve direct stellar diameter measurements from ground-based interferometry or satellite projects such as GAIA, which is designed to measure at the 10μas level (Bastian & Schilbach 1996). More refined data of this kind will cause a major improvement in the fundamental parameters of cool dwarf stars.

Acknowledgements. We like to thank Jan Bernkopf for valuable discussions on the evolutionary status of Procyon. Several suggestions of the referee are gratefully acknowledged. This research was supported by the *BMBF* under grant 05 2MU114 7 and partly by the *Deutsche Forschungsgemeinschaft, DFG* under grant Ge 490/9-2.

References

Adams, W.S., Kohlschütter, A. 1914, ApJ 39, 341
Anders, E., Grevesse, N. 1989, Geochim. Cosmochim. Acta 53, 197
Anstee, S.D., O'Mara, B.J. 1995, MNRAS 276, 859
Bastian, U., Schilbach, E. 1996, Rev. Mod. Astron. 9, 87
Beeckmans, F. 1977, A&A 60, 1
Bell, R.A., Paltoglou, G., Tripicco, M.J. 1994, MNRAS 268, 771
Biémont, E., Baudoux, M., Kurucz, R.L., Ansbacher, W., Pinnington, E.H. 1991, A&A 249, 539
Blackwell, D.E., Shallis, M.J. 1977, MNRAS 180, 177
Blackwell, D.E., Willis, R.B. 1977, A&A 180, 169
Blackwell, D.E., Booth, A.J., Petford, A.D. 1984, A&A 132, 236
Blackwell, D.E., Smith, G., Lynas-Gray, A.E. 1995, A&A 303, 575
Castelli, F., Gratton, R.G., Kurucz, R.L. 1996, A&A in press
Cayrel, G., Cayrel, R. 1963, ApJ 137, 431
Cayrel de Strobel, G. 1969, *Theory and observation of normal stellar atmospheres*, ed. O. Gingerich, Cambridge, p. 35
Chamberlain, J.W., Aller, L.H.: 1951, ApJ 114, 52
Chang, T.N. 1990, Phys. Rev. A 41, 4922
Code, A.D., Davis, J., Bless, R.C., Hanbury Brown, R. 1976, ApJ 203, 417
Drake, J.J., Smith, G. 1991, MNRAS 250, 89
Drake, J.J., Smith, G. 1993, ApJ 412, 797
Dravins, D. 1987, A&A 172, 211
Dyson, S.E., Girard, T.M., van Altena, W.F. 1994, BAAS 26, 929
Edvardsson, B. 1988a, *The impact of very high S/N spectroscopy on stellar physics*, IAU Symp. 132, eds. G. Cayrel de Strobel and M. Spite, Kluwer, p. 387
Edvardsson, B. 1988b, A&A 190, 148
Fuhrmann, K., Axer, M., Gehren, T. 1993, A&A 271, 451
Gehren, T. 1977, A&A 59, 303
Gray, D.F. 1977, ApJ 218, 530
Gray, D.F. 1981a, ApJ 251, 152
Gray, D.F. 1981b, ApJ 251, 583
Gray, D.F. 1992, *The observation and analysis of stellar photospheres*, Cambridge Univ. Press
Grevesse, N. 1991, *Evolution of stars: the photospheric abundance connection*, IAU Symp. 145, eds. G. Michaud and A. Tutukov, Kluwer, p. 63
Grevesse, N., Noels, A. 1993, *Origin and evolution of the elements*, eds. N. Prantzos et al., Cambridge Univ. Press, p. 14
Griffin, R. and R. 1979, *A photometric atlas of the spectrum of Procyon*, Cambridge
Hanbury Brown, R., Davis, J., Allen, L.R. 1974, MNRAS 167, 121
Hannaford, P., Lowe, R.M., Grevesse, N., Noels, A. 1992, A&A 259, 301
Holweger, H., Heise, C., Kock, M. 1990, A&A 232, 510
Holweger, H., Bard, A., Kock, A., Kock, M. 1991, A&A 249, 545
Holweger, H., Kock, M., Bard, A. 1995, A&A 296, 233
Horne, K. 1986, PASP 98, 609
Irwin, A.W., Fletcher, J.M., Yang, S.L.S., Walker, G.A.H. Goodenough, C. 1992, PASP 104, 489
Kostik, R.I., Shchukina, N.G., Rutten, R.J. 1996, A&A 305, 325
Kurucz, R.L. 1979, ApJS 40, 1
Kurucz, R.L. 1992a, Rev. Mex. Astron. Astrofis. 23, 45
Kurucz, R.L. 1992b, Rev. Mex. Astron. Astrofis. 23, 181
Kurucz, R.L. 1995a, ApJ 452, 102
Kurucz, R.L. 1995b, Highlights of Astronomy 10, 407
Kurucz, R.L. 1995c, *Astrophysical Applications of Powerful New Databases*, eds. S.J. Adelman and W.L. Wiese, ASP Conf. Ser. 78, 205
Kurucz, R.L., Furenlid, I., Brault, J., Testerman, L. 1984, *Solar Flux Atlas from 296 to 1300 nm*, KPNO, Tucson

Magain, P., Zhao, G. 1996, A&A 305, 245
Milford, P.N., O'Mara, B.J., Ross, J.E. 1994, A&A 292, 276
Mozurkewich, D., Johnston, K.J., Simon, R.S., Bowers, P.F., Gaume, R., Hutter, D.J., Colavita, M.M., Shao, M., Pan, X.P. 1991, AJ 101, 2207
Nave, G., Johansson, S. 1993a, A&A 274, 961
Nave, G., Johansson, S. 1993b, A&AS 102, 269
Pfeiffer, M., Frank, C., Gehren, T. 1996, A&A in preparation
Smalley, B., Dworetsky, M.M. 1995, A&A 293, 446
Smith, G., Drake, J.J. 1987, A&A 181, 103
Smith, G., Edvardsson, B., Frisk, U. 1986, A&A 165, 126
Smith, G., Lambert, D.L., Ruck, M.J. 1992, A&A 263, 249
Steffen, M. 1985, A&AS 59, 403
Walker, G.A.H., Walker, A.R., Racine, R., Murray Fletcher, J., McClure, R.D. 1994, PASP 106, 356
Watanabe, T., Steenbock, W. 1985, A&A 149, 21
Wiese, W.L., Smith, M.W., Miles, B.M. 1969, *Atomic transition probabilities*, Vol. II, NSRDS-NBS 22, Washington, D. C.

This article was processed by the author using Springer-Verlag LaTeX A&A style file *L-AA* version 3.